Internal Note 69-FM-83

NATIONAL AERONAUTICS AND SPACE ADMINISTRATION

MSC INTERNAL NOTE NO. 69-FM-83

APRIL 14, 1969

APOLLO 10 (MISSION F)
(AS-505/CSM 106/LM-4)
SPACECRAFT DISPERSION ANALYSIS
VOLUME I
NAVIGATION ERROR ANALYSIS

APR 22 1969
Technical Library, Bellcomm, Inc.
FEB 1974 RECEIVED NASA STI FACILITY INPUT BRANCH

Mathematical Physics Branch

MISSION PLANNING AND ANALYSIS DIVISION

MANNED SPACECRAFT CENTER
HOUSTON, TEXAS

(NASA-TM-X-69796) APOLLC 10 (MISSION F) (AS-505/CSM-106/LM-4) SPACECRAFT DISPERSION ANALYSIS. VOLUME 1: NAVIGATION ERROR ANALYSIS (NASA) 39 p

N74-70712

Unclas
00/99 16419

MSC INTERNAL NOTE NO. 69-FM-83

PROJECT APOLLO

APOLLO 10 (MISSION F) (AS-505/CSM-106/LM-4) SPACECRAFT DISPERSION ANALYSIS VOLUME I - NAVIGATION ERROR ANALYSIS

By L. R. Lewis
J. R. Mellon
G. D. Petzel
Navigation Analysis Section
TRW Systems Group

April 14, 1969

MISSION PLANNING AND ANALYSIS DIVISION
NATIONAL AERONAUTICS AND SPACE ADMINISTRATION
MANNED SPACECRAFT CENTER
HOUSTON, TEXAS

MSC Task Monitor
Paul Mitchell

Approved: E R Robinson for
J. C. McPherson, Chief
Mathematical Physics Branch

Approved: D H Owen
for John P. Mayer, Chief
Mission Planning and Analysis Division

CONTENTS

Section		Page
1.	SUMMARY	1
2.	INTRODUCTION	3
2.1	Error Model	3
2.2	Navigation Plan	3
2.2.1	Phase I	4
2.2.2	Phase II	4
2.2.3	Phase III	5
3.	SYMBOLS	7
4.	RESULTS	9
5.	CONCLUSIONS	11
	REFERENCES	35

TABLES

Table		Page
I	One-Sigma Values of MSFN Error Sources	13
II	Three-Sigma Earth Parking Orbit Uncertainties	14
III	Three-Sigma Translunar Uncertainties	14
IV	Three-Sigma Transearth Uncertainties	15
V	One-Sigma Covariance Matrices	16

FIGURES

Figure		Page
1	F-Mission Event Schedule	23
2	Tracking Schedule for Earth Parking Orbit Phase	24
3	Tracking Schedule for Translunar Phase	25
4	Tracking Schedule for Transearth Phase	26
5	Three-Sigma Local Position Uncertainty - Translunar Phase	27
6	Three-Sigma Local Velocity Uncertainty - Translunar Phase	28
7	Three-Sigma Predicted Pericynthion Altitude Uncertainty - Translunar Phase	29
8	Three-Sigma Local Position Uncertainty - Transearth Phase	30
9	Three-Sigma Local Velocity Uncertainty - Transearth Phase	31
10	Three-Sigma Predicted Radial Velocity Uncertainty at Entry - Transearth Phase	32
11	Three-Sigma Predicted Flight-Path Angle Uncertainty at Fixed Entry Radius - Transearth Phase	33

APOLLO 10 (MISSION F) (AS-505/CSM-106/LM-4)

SPACECRAFT DISPERSION ANALYSIS

VOLUME I - NAVIGATION ERROR ANALYSIS

By L. R. Lewis
J. R. Mellon
G. D. Petzel
Navigation Analysis Section
TRW Systems Group

1. SUMMARY

An error analysis of simulated observations by MSFN stations has been performed to determine an estimate of the accuracy of the ground differential correction scheme at specific times during the F mission. Local uncertainties in the spacecraft position and velocity vectors are presented for the earth parking orbit and the translunar and transearth coast phases. Also presented are the uncertainties in pericynthion altitude during the translunar phase, the flight-path angle at fixed entry radius, and radial velocity at entry during the transearth phase.

The navigation analysis of the lunar orbit and rendezvous phases of the F mission was not completed in time for inclusion in this document. The delay was caused by the lack of a technique to perform a complete analysis consistent with the observed navigation accuracies obtained from postflight analysis of Lunar Orbiter 3 and Apollo 8. A technique is now available and the analysis of the lunar orbit and rendezvous phases will be published as an addendum to this document.

Based on the analysis presented, the MSFN provides adequate navigation for the earth parking orbit and the translunar and transearth phases of the F mission.

2. INTRODUCTION

The navigation analysis is based on the reference trajectory described in Reference 1. The purpose of this analysis is to compute an estimate of the accuracy with which the F mission trajectories can be determined from MSFN tracking data. This information is used to support a complete dispersion analysis for the F mission that computes an estimate of the fuel required to satisfy the mission objectives as well as the expected trajectory dispersions. The analysis simulates the data incorporation and filtering techniques that may be employed by the RTCC.

The computer programs used for conducting the analysis are described below:

a. TAPP-IV generates an integrated trajectory which matches the reference trajectory. This program performs a complete tracking simulation for the mission including the generation of the trajectory, vehicle rise-set times, tracking information matrices when given input stations, their associated data types and rates, and coordinate transformation and state transition matrices (Reference 2).

b. MOFIT and SNAP use the information from the TAPP-IV tape to compute the accuracies using a linear error analysis technique (References 3 and 4).

2.1 Error Model

The error sources considered in the generation of the ground tracking information matrices are the noise and bias on each data type, the uncertainties in station location for each station, the uncertainty in the earth gravitational constant, the uncertainty in the moon gravitational constant (TL and TE coast phases), and the S-IVB venting uncertainty (EPO coast phase). Table I lists the one-sigma values for each of the above error sources. These values are associated with a Gaussian distribution with zero mean.

2.2 Navigation Plan

The navigation plan consists of an observation schedule and specifications for using the resultant data. An error analysis, based on the navigation plan, provides an assessment of the effect of tracking and orbit prediction errors on the accuracy of orbit determination.

The assumed MSFN tracking schedule includes USB stations only. The following guidelines are used in the development of the tracking plan:

a. Two or more stations do not track the vehicle simultaneously during the earth parking orbit phase.

b. The ground update for TLI occurs at least 30 minutes prior to the maneuver. At least 10 minutes before an update, all tracking must have been completed for that update.

c. Only one triad of stations at a time tracks the vehicle during the translunar and transearth coast phases (i.e., three-way doppler, one master, two slaves).

d. Tracking must occur above the 5-degree elevation angle.

e. Tracking does not occur when the CSM high-gain antenna is occulted from the earth.

The data types considered for the earth parking orbit phase are two-way doppler and X-/Y-angles at a rate of one set of observations per 6 seconds. During the translunar and transearth coast phases, two-way doppler observations are simulated for the master station, and three-way doppler is simulated for the other two stations (slave stations) in the triad. The data rate is one set of observations per minute except for periods when the CSM high-gain antenna is assumed occulted as a result of CSM thermal roll.

The description of the mission is discussed below in three phases:

Phase I EPOI to S-IVB reignition

Phase II TLI to pericynthion

Phase III TEI to entry

Figure 1 is an event schedule which presents the order of the MSFN updates and times of the maneuvers.

2.2.1 Phase I. - The assumed lift-off time for the trajectory simulation is May 17, 1969, 16:33:49.371 (hr:min:sec) GMT. The launch phase is completed at S-IVB cutoff, 11:21.566 (min:sec) g.e.t., at which time the S-IVB/CSM/LM is inserted into a 100-nautical mile circular parking orbit. The nominal TLI opportunity occurs upon S-IVB reignition at 2:31:36.373 (hr:min:sec) g.e.t. The update for the maneuver is assumed to be sent from CYI approximately 38 minutes prior to TLI. The second TLI opportunity occurs approximately 88 minutes after the nominal opportunity. The update for this maneuver is assumed to be sent from ACN approximately 30 minutes prior to the maneuver. Figure 2 presents the bar graph of the tracking schedule used during Phase I.

2.2.2 Phase II. - The reference trajectory TLI maneuver is targeted for a pericynthion altitude of approximately 60 nautical miles and earth return vacuum perigee of approximately 20 nautical miles, which results in a free return circumlunar trajectory. TLI burnout was assumed to

occur at 2:36:43.37 (hr:min:sec) g.e.t. The timeline is designed to have four midcourse corrections which occur at 7 and 24 hours after TLI and 22 and 5 hours prior to LOI. The updates for the midcourse corrections are assumed to occur 2 hours prior to each MCC. The LOI maneuver inserts the spacecraft into an elliptical lunar orbit (60 by 170 nautical miles) at 76:8:17.58 (hr:min:sec) g.e.t.

The time from TLI to pericynthion is approximately 73:40 (hr:min). Figure 3 is a bar graph of the tracking schedule used for the analysis during Phase II. The blackened station in each triad is the master station. There is no tracking during those periods when the high-gain antenna of the CSM is assumed occulted as a result of the passive thermal control constraint. The passive thermal control constraint is assumed to be initiated 3 hours after TLI, discontinued from 1 hour before to 1/2 hour after each midcourse correction, and terminated 3 hours prior to pericynthion (Reference 5).

2.2.3 Phase III. - Transearth injection was assumed to occur on May 23, 1969 at 28:3.741 (min:sec) GMT, with earth entry approximately 63.4 hours later. Thermal roll is simulated on the transearth trajectory beginning 2 hours after TEI and ending 2-1/2 hours prior to earth entry. Exceptions during this time are periods beginning 1 hour before each of the assumed midcourse correction times (TEI plus 15 hours, entry minus 15 hours, and entry minus 3 hours) and ending 1/2 hour after MCC time. Updates for the midcourse corrections are assumed to occur 2 hours prior to each MCC. Figure 4 presents the bar graph of the tracking schedule used during Phase III. The blackened station in each triad is the master station.

3. SYMBOLS

ACN	Ascension Island
ANG	Antigua Island
BDA	Bermuda Island
CNB	Canberra, Australia
CRO	Carnarvon, Australia
CSM	command and service module
CYI	Grand Canary Island
EPOI	earth parking orbit insertion
GBM	Grand Bahama Island
GDS	Goldstone, California
g. e. t.	ground elapsed time
GMT	Greenwich mean time
GWM	Guam
GYM	Guaymas, Mexico
HAW	Kauai, Hawaii
h_{pc}	pericynthion altitude
h_{pg}	vacuum perigee altitude
LM	lunar module
LOI	lunar orbit insertion
MAD	Madrid, Spain
MCC	midcourse correction
MIL	Merritt Island
MSA	moon's sphere of action

MSFN	Manned Spaceflight Network
RSS	root-sum-square
RTCC	Real Time Computing Center
SPS	service propulsion system
S-IVB	Saturn IVB
TEI	transearth injection
TEX	Corpus Christi, Texas
TLI	translunar injection
USB	unified S-band
$\dot{U}$	radial component of velocity
γ	flight-path angle

4. RESULTS

The values presented in Figures 5 through 11 and Tables II through IV are defined as three-sigma uncertainties. These values were calculated by taking the square root of the variance (sum of the variances for the three components of position and velocity uncertainties, respectively) for the particular parameter and multiplying the resulting value by three.

The three-sigma uncertainties from this analysis for the translunar and transearth phases are presented in Figures 5 through 11 The local position and velocity uncertainties (Figures 5, 6, 8, and 9) are plotted as a function of elapsed time from TLI or TEI. All available MSFN tracking data accumulated up to, and including, that time were used to compute the uncertainties. The predicted pericynthion altitude, radial velocity, and flight-path angle uncertainties (figures 7, 10, and 11) are the accuracies at the elapsed time from injection propagated to pericynthion (for h_{pc}) or earth entry (for $\dot{u}$ and γ). Table II lists specific accuracies for position, velocity, and predicted altitude (at nominal time of pericynthion arrival) during the translunar phase. Table IV lists specific accuracies for position, velocity, flight-path angle at fixed entry radius, and radial velocity at entry during the transearth phase.

The three-sigma position uncertainties for the TL coast phase reached a maximum of 12.6 nautical miles at 56 hours after injection and decreased to about 3.4 nautical miles at pericynthion. The three-sigma velocity uncertainties decreased to a minimum of 0.15 foot per second at 5 hours prior to pericynthion and increased to its maximum of 27 feet per second at pericynthion. The predicted pericynthion altitude uncertainties reached a maximum of 12.5 nauticial miles at 10 hours after injection, decreased to 7.3 nautical miles at TLI plus 20 hours, remained fairly constant to TLI plus 55 hours, and then dropped sharply to 0.54 nautical mile at pericynthion. The three-sigma position uncertainties for the TE coast phase decreased from a maximum of 28 nautical miles after 2 hours of tracking to a minimum of 0.3 nautical mile at entry. The three-sigma velocity uncertainties decreased to a minimum of 0.39 foot per second at 8 hours prior to entry and increased to 2.6 feet per second at entry. The three-sigma radial velocity uncertainties at entry decreased from 3000 feet per second after 1 hour of tracking to a minimum of 1.1 feet per second at entry. The three sigma flight-path angle uncertainties at fixed entry radius decreased from 5.7 degrees after 1 hour of tracking to 0.009 degree at entry.

The one-sigma covariance matrices representing the estimated accuracy associated with the spacecraft position and velocity vectors at the time of TLI-1 and TLI-2, midcourse corrections, LOI, and entry are presented in Table V. These matrices are referenced to a u, v, w (orbit plane) coordinate system relative to the CSM at the indicated event.

5. CONCLUSIONS

Based on the MSFN capabilities in the determination of the F mission trajectories studied, the following conclusion is made:

> The results obtained from this analysis indicate that the MSFN navigation is adequate for the various phases studied.

Table I. One-Sigma Values of MSFN Error Sources

USB Station Tracking Accuracy

Phase	Noise	Bias
EPO Phase		
X-Y angles	0.8E-3 rad	1.6E-3 rad
Two-way doppler (1 per 6 sec)	0.02 ft/sec	0.03 ft/sec
TL & TE Coast Phases		
Two-way doppler (1 per 60 sec)	0.002 ft/sec	0.03 ft/sec
Three-way doppler	0.002 ft/sec	0.03 ft/sec

Station Location Uncertainties

Station	Longitude (rad)	Latitude (rad)	Altitude (ft)
GBM	0.58177643E-5	0.48481369E-5	134.51444
BDA	0.62873917E-5	0.58177643E-5	141.07612
ANG	0.58177643E-5	0.53329506E-5	137.79528
CYI	2.4725498E-5	2.2301430E-5	104.98688
ACN	1.6968479E-5	1.6483666E-5	104.98688
MAD	0.38785094E-5	0.48481369E-5	141.07612
CRO	1.0665901E-5	0.92114602E-5	216.53543
GWM	3.1997704E-5	3.1028076E-5	104.98688
CNB	1.0665901E-5	0.92114602E-5	216.53543
HAW	0.77570191E-5	0.67873917E-5	141.07612
GDS	0.58177643E-5	0.53329506E-5	131.23360
GYM	0.58177643E-5	0.48481369E-5	134.51444
TEX	0.53329506E-5	0.48481369E-5	131.23360
MIL	0.58177643E-5	0.48481369E-5	131.23360

Uncertainty in earth gravitational constant: 1.06E11 ft^3/sec^2

Uncertainty in moon gravitational constant: 7.1E9 ft^3/sec^2

S-IVB venting: 10% of venting magnitude described in Reference 6.

Table II. Three-Sigma Earth Parking Orbit Uncertainties

Event	Position Uncertainty RSS (n mi)	U (ft)	V (ft)	W (ft)	Velocity Uncertainty RSS (ft/sec)	U (ft/sec)	V (ft/sec)	W (ft/sec)
TLI-1	3.89	4,200	22,700	4,300	26.19	25.83	2.50	3.44
TLI-2	5.89	8,900	34,500	2,700	39.54	38.82	7.38	1.54

Table III. Three-Sigma Translunar Uncertainties

Event	Position Uncertainty RSS (n mi)	U (ft)	V (ft)	W (ft)	Velocity Uncertainty RSS (ft/sec)	U (ft/sec)	V (ft/sec)	W (ft/sec)	Predicted h_{pc} Uncertainty (n mi)
MCC-1	7.76	1,400	21,800	41,800	1.16	0.17	0.64	0.95	9.64
MCC-2	8.36	4,500	40,600	30,100	0.43	0.05	0.32	0.29	7.87
MCC-3	11.94	8,500	58,000	42,700	0.27	0.04	0.19	0.18	6.93
MCC-4	9.84	12,100	14,000	56,900	0.15	0.08	0.02	0.12	2.00
LOI*	4.95	9,100	15,200	24,300	24.22	9.72	3.53	21.90	1.5

*These values are the uncertainties at the LOI update (LOI minus 2:15 (hr:min)) propagated to LOI.

Note: The values at MCC-4 and LOI are referenced to the moon and the values at all other events in the above two tables are referenced to the earth.

Table IV. Three-Sigma Transearth Uncertainties

Event	Position Uncertainty RSS (n mi)	Position Uncertainty U (ft)	Position Uncertainty V (ft)	Position Uncertainty W (ft)	Velocity Uncertainty RSS (ft/sec)	Velocity Uncertainty U (ft/sec)	Velocity Uncertainty V (ft/sec)	Velocity Uncertainty W (ft/sec)	Predicted Entry γ at Fixed Radius Uncertainty (deg)	Predicted Entry $\dot{U}$ Uncertainty (ft/sec)
MCC-5	24.19	1,500	54,000	136,600	3.20	0.04	1.01	3.03	0.75	372
MCC-6	12.74	4,500	27,100	72,400	0.54	0.04	0.14	0.52	0.13	51
MCC-7	5.94	3,500	12,200	33,700	0.73	0.09	0.20	0.68	0.07	12
Entry*	1.01	3,600	4,500	2,100	8.85	3.93	2.79	7.44	0.04	4

*These values are the uncertainties at the entry update (entry minus 1 hour) propagated to entry.
Note: All values in the above table are referenced to the earth.

Table V. One-Sigma Covariance Matrices

Format:

σ_{uu}

σ_{uv} σ_{vv}

σ_{uw} σ_{vw} σ_{ww} symmetrical

$\sigma_{u\dot{u}}$ $\sigma_{v\dot{u}}$ $\sigma_{w\dot{u}}$ $\sigma_{\dot{u}\dot{u}}$

$\sigma_{u\dot{v}}$ $\sigma_{v\dot{v}}$ $\sigma_{w\dot{v}}$ $\sigma_{\dot{u}\dot{v}}$ $\sigma_{\dot{v}\dot{v}}$

$\sigma_{\dot{u}\dot{w}}$ $\sigma_{v\dot{w}}$ $\sigma_{w\dot{w}}$ $\sigma_{\dot{u}\dot{w}}$ $\sigma_{\dot{v}\dot{w}}$ $\sigma_{\dot{w}\dot{w}}$

Coordinate System:

u - in the direction of the geocentric or selenocentric radius vector of the vehicle at the time of the event

v - orthogonal to u, pointing downrange in the orbit plane

w - mutually orthogonal to u and v, completing the right-handed system

The units for position and velocity are feet and feet per second, respectively.

One-Sigma Covariance of S-IVB/CSM/LM*
TLI-1

	1	2	3	4	5	6
1	.19310517+07					
2	-.10498816+08	.57436065+08				
3	.19470219+07	-.10620967+08	.20314880+07	Symmetrical		
4	.11926097+05	-.65237831+05	.12070881+05	.74103697+02		
5	-.11515467+04	.62845907+04	-.11659639+04	-.71389141+01	.69504346-00	
6	.15450447+04	-.84146593+04	.16176338+04	.95629505+01	-.92537552-00	.13130109+01

One-Sigma Covariance of S-IVB/CSM/LM*
TLI-2

	1	2	3	4	5	6
1	.87929740+07					
2	-.34122256+08	.13255185+09				
3	.26272493+07	-.10204741+08	.79602379+06	Symmetrical		
4	.38343257+05	-.14894768+06	.11466358+05	.16737497+03		
5	-.72919620+04	.28319702+05	-.21809974+04	-.31822316+02	.60589162+01	
6	.14292507+04	-.55514181+04	.43995415+03	.62356357+01	-.11868773+01	.26463185-00

*Earth central body

One-Sigma Covariance of CSM/LM*
TLI+7 hours (MCC-1)

	1	2	3	4	5	6
1	.23211684+06					
2	.14559346+06	.52743885+08		Symmetrical		
3	.34811332+07	-.31603817+08	.19375024+09			
4	.96699829+01	-.36973885+03	.48733170+03	.33740029-02		
5	.67506041+01	.15479222+04	-.91124866+03	-.10942219-01	.45777044-01	
6	.73163240+02	-.18153992+03	.40899054+04	.74712846-02	-.63907158-02	.10112392+00

One-Sigma Covariance of CSM/LM*
TLI+24 hours (MCC-2)

	1	2	3	4	5	6
1	.22580455+07					
2	.15395111+08	.18358409+09		Symmetrical		
3	.54778247+07	.22360504+08	.10040396+09			
4	.31987505+01	-.99587759+02	.56678519+02	.31566513-03		
5	.12151210+03	.14182355+04	.17281128+03	-.82296357-03	.11049010-01	
6	.54953645+02	.57967199+03	.69982306+03	.20587999-03	.40146054-02	.92931751-02

*Earth central body

One-Sigma Covariance of CSM/LM*
LOI - 22 hours (MCC-3)

	1	2	3	4	5	6
1	.80199155+07					
2	.41723900+08	.37437235+09			Symmetrical	
3	.61667764+07	.70916473+07	.20242190+09			
4	.10457189+02	-.76219082+02	.57729089+02	.20630029-03		
5	.13829903+03	.12290582+04	.70324405+01	-.29791101-03	.40827017-02	
6	.27167516+02	.21217366+03	.65856142+03	.28869436-03	.41530795-03	.37619956-02

One-Sigma Covariance of CSM/LM**
LOI - 5 hours (MCC-4)

	1	2	3	4	5	6
1	.16252429+08					
2	.12624224+08	.21631883+08			Symmetrical	
3	.18869936+08	.41694828+08	.35951198+09			
4	.87534438+02	.51831920+02	.20658609+03	.74740790-03		
5	-.17555191+02	-.91157749+01	-.94466712+02	-.15187152-03	.59810272-04	
6	-.95186428+02	-.97334141+02	-.20677999+03	-.50757200-03	.51029833-04	.17231935-02

*Earth central body

**Moon central body

One-Sigma Covariance of CSM/LM*
LOI Update (LOI - 2 hours, 15 minutes) Propagated to LOI

	1	2	3	4	5	6
1	.91922777+07					
2	-.11651372+08	.25512493+08		Symmetrical		
3	.14745207+08	-.21475622+08	.65757387+08			
4	.85290052+04	-.16080474+05	.15178001+05	.10503433+02		
5	-.34325459+04	.33560835+04	-.55616169+04	-.27045797+01	.13857574+01	
6	-.13363104+05	.19536205+05	-.59187630+05	-.13792070+02	.50327340+01	.53282131+02

One-Sigma Covariance of CSM**
TEI + 15 hours (MCC-5)

	1	2	3	4	5	6
1	2.6607021+05					
2	3.0075577+06	3.2408234+08		Symmetrical		
3	3.0276243+06	7.1396621+08	2.0767038+09			
4	5.5711742+00	-2.7729327+01	-2.5503350+02	1.9067870-04		
5	4.1452654+01	5.0924551+03	1.3930427+04	-1.0460708-03	1.1388343-01	
6	2.0777614+01	1.1338952+04	4.1022313+04	-6.2377819-03	3.1111784-01	1.0208613+00

*Moon central body

**Earth central body

One-Sigma Covariance of CSM*
Entry - 15 hours (MCC-6)

	1	2	3	4	5	6
1	2.2499648+06					
2	7.1488293+06	8.1505532+07			Symmetrical	
3	2.6332852+06	-7.1105521+06	5.8253612+08			
4	6.6597383+00	-6.0280771+01	9.3184922+01	1.8984496-04		
5	-4.9855360+00	9.2183721+01	3.1460284+02	-1.4334124-04	2.2197093-03	
6	-6.6301678+01	-4.8246340+02	2.8602291+03	5.1589209-04	6.1502936-03	3.0340813-02

One-Sigma Covariance of CSM*
Entry - 3 hours (MCC-7) vl

	1	2	3	4	5	6
1	1.3572087+06					
2	-6.4756230+05	1.6522461+07			Symmetrical	
3	-7.9472174+05	-2.9889361+05	1.2647253+08			
4	2.8553671+01	-2.3532889+02	5.8447625+01	3.9633099-03		
5	3.6643645+00	-2.0988664+02	1.4286683+02	3.4830552-03	4.5933013-03	
6	3.0606469+00	1.7623322+02	-2.1079440+03	-2.0172364-03	3.8939161-04	5.1029374-02

*Earth central body

One-Sigma Covariance of CSM*
Entry Update (Entry - 1 hour) Propagated to Entry

	1	2	3	4	5	6
1	1.4204682+06				Symmetrical	
2	-2.5147619+05	2.3064465+06				
3	-4.5184957+04	1.9848775+05	4.7796785+05			
4	4.9228926+02	-1.9449496+03	-1.4444184+02	1.7037807+00		
5	-1.0755304+03	-1.5848637+02	1.9496076+01	-8.4924516-02	8.7231232-01	
6	7.5465269+02	-8.7325323+02	-1.5346350+03	8.5221028-01	-4.8577971-01	6.1413188+00

*Earth central body

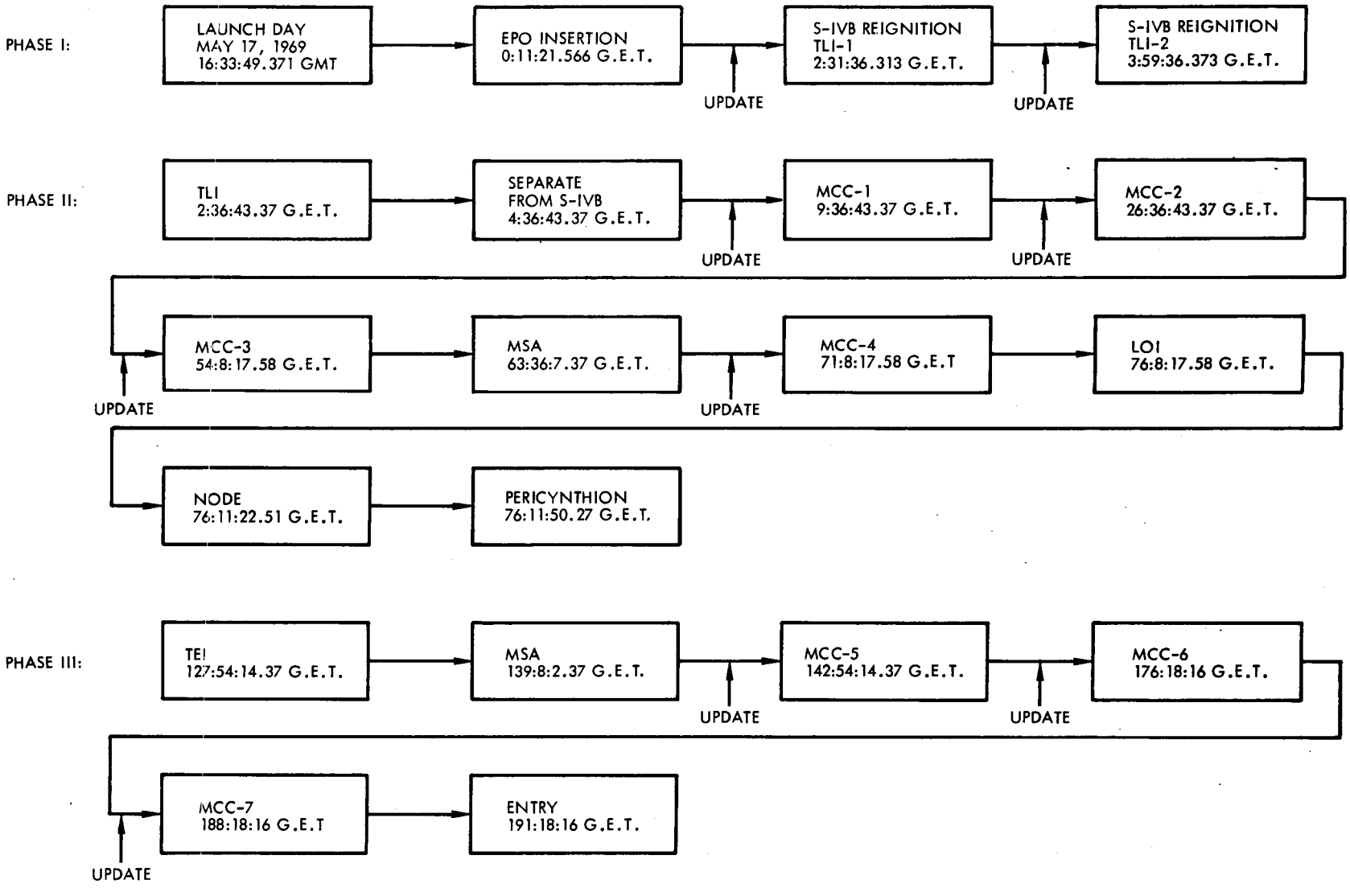

Figure 1. F-Mission Event Schedule

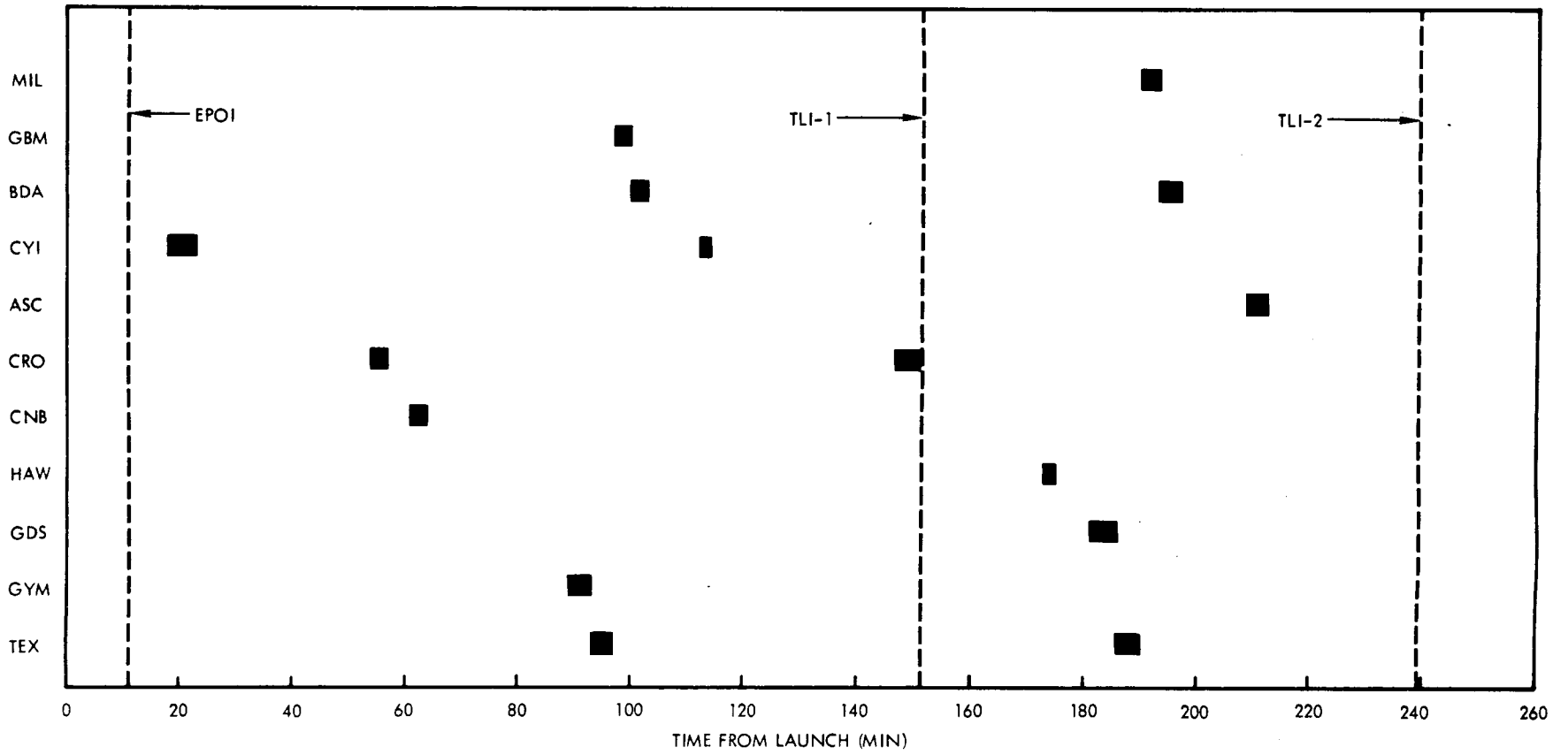

Figure 2. Tracking Schedule for Earth Parking Orbit Phase

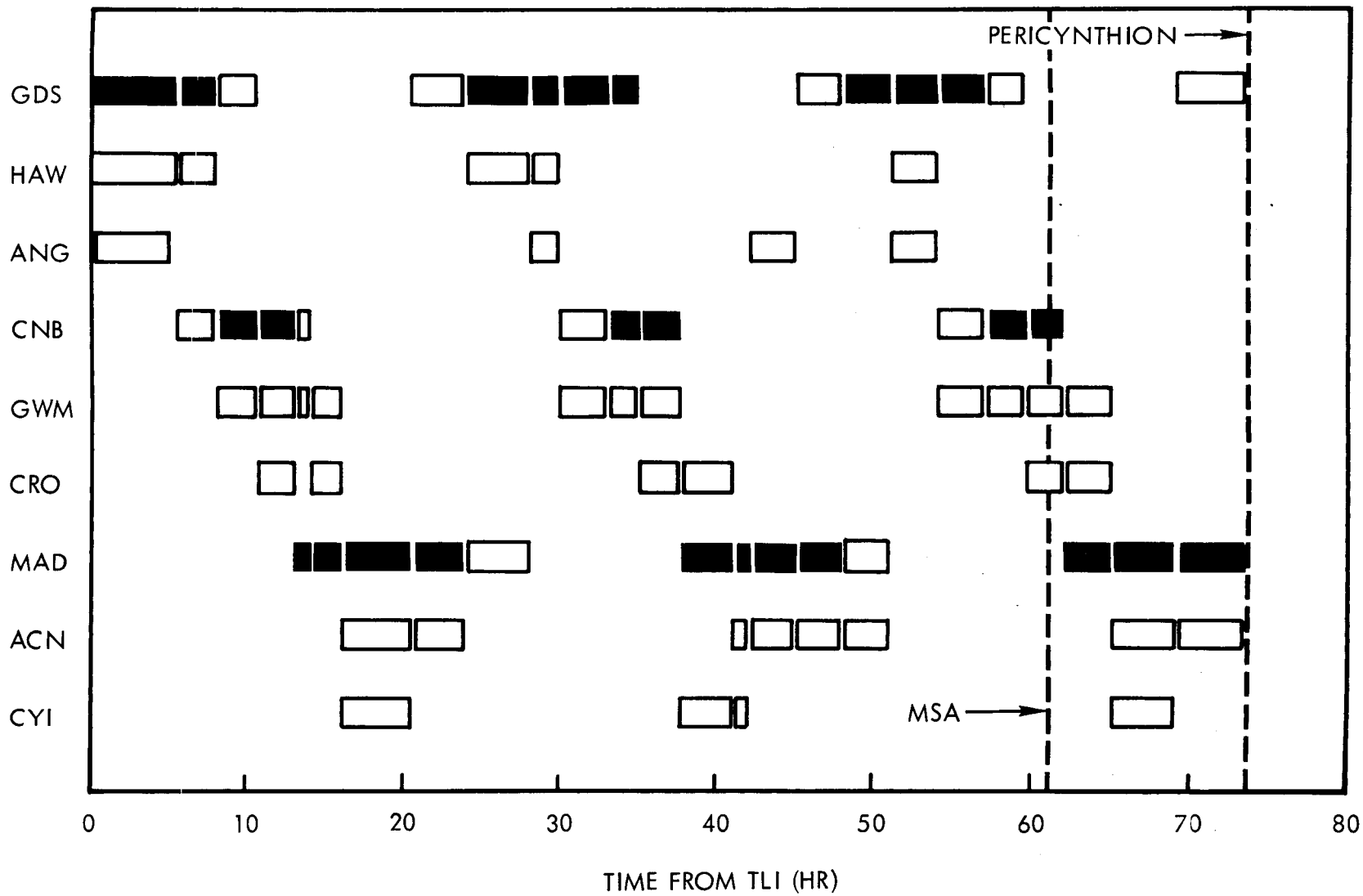

Figure 3. Tracking Schedule for Translunar Phase

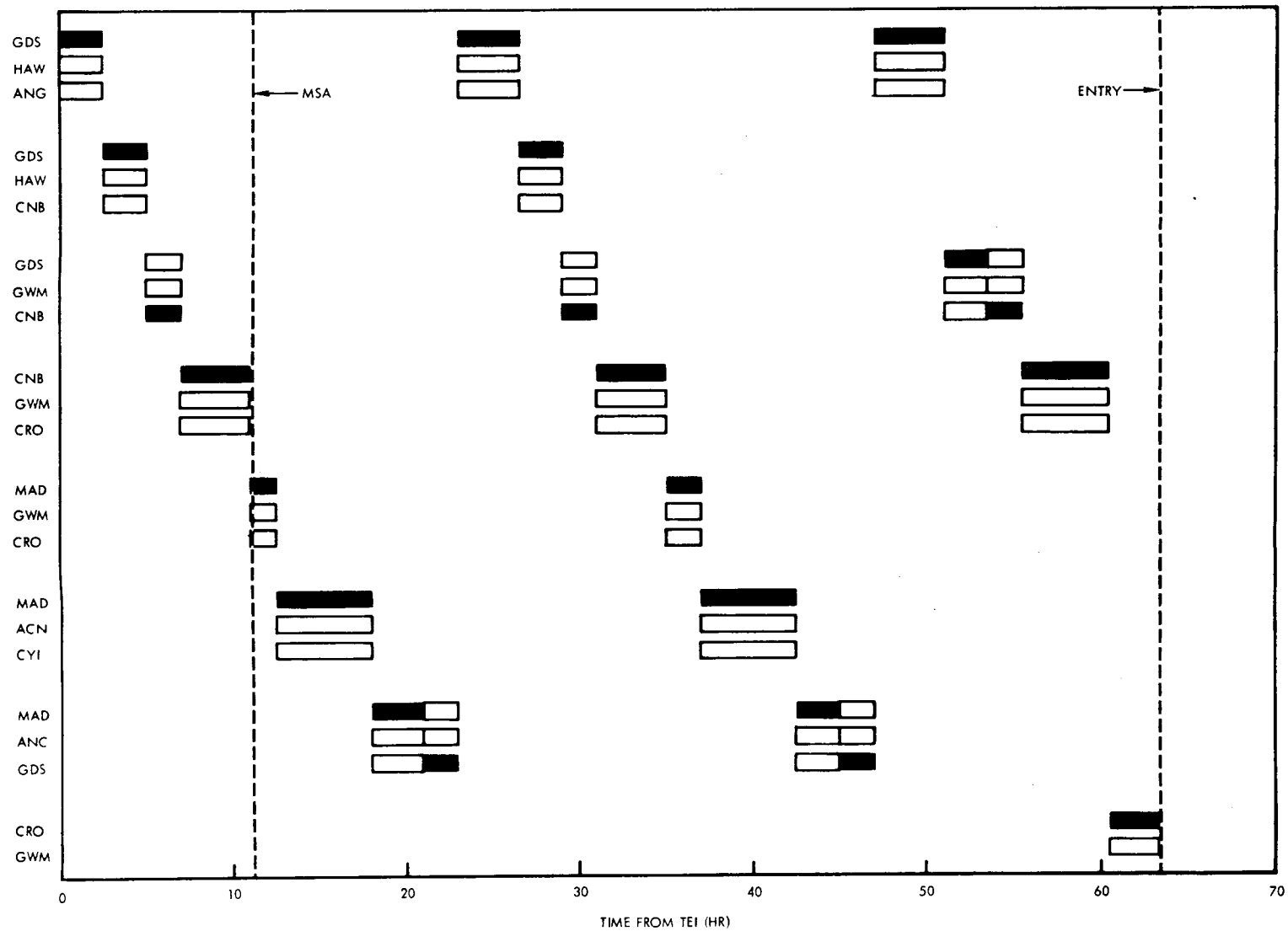

Figure 4. Tracking Schedule for Transearth Phase

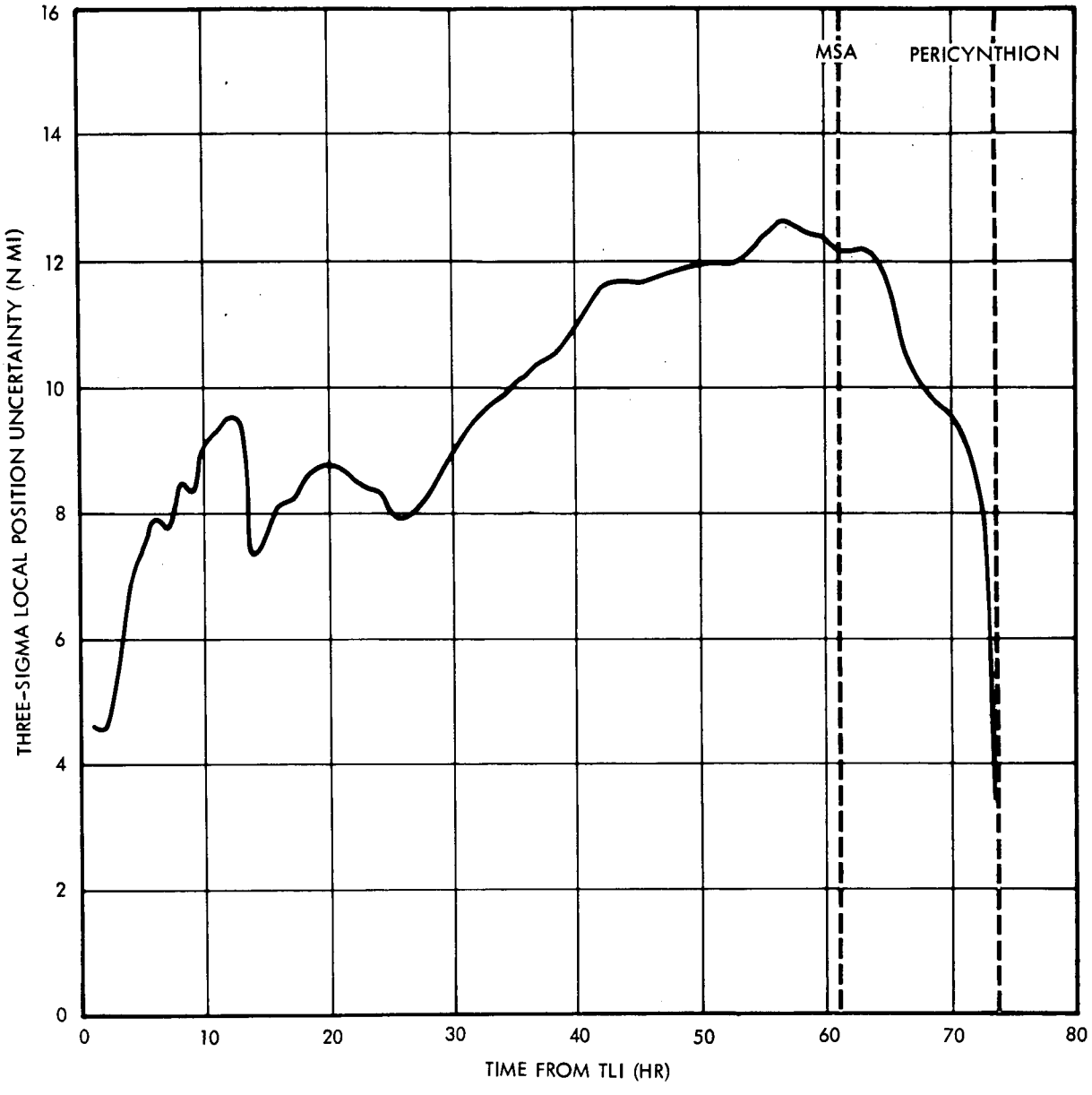

Figure 5. Three-Sigma Local Position Uncertainty - Translunar Phase

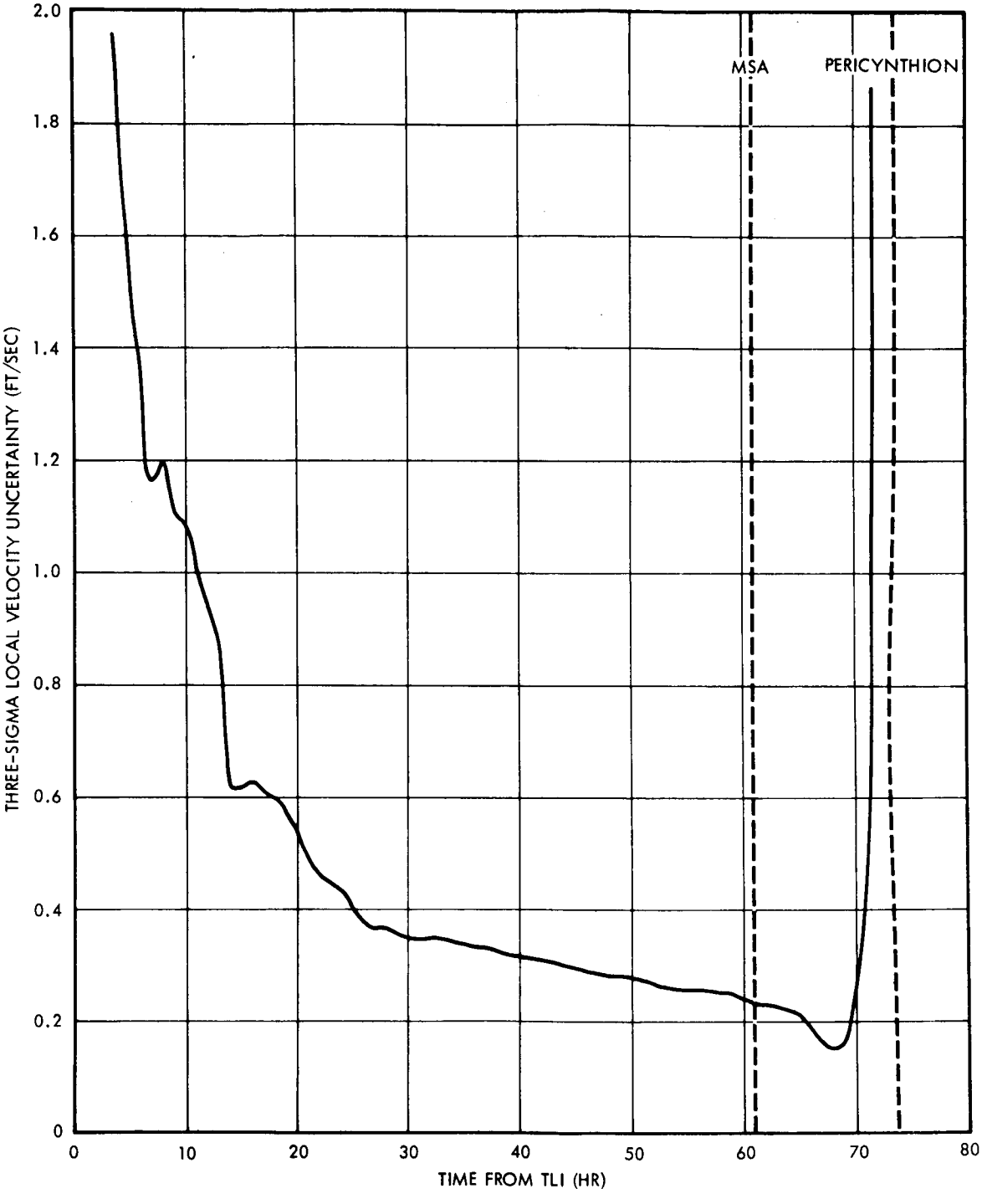

Figure 6. Three-Sigma Local Velocity Uncertainty - Translunar Phase

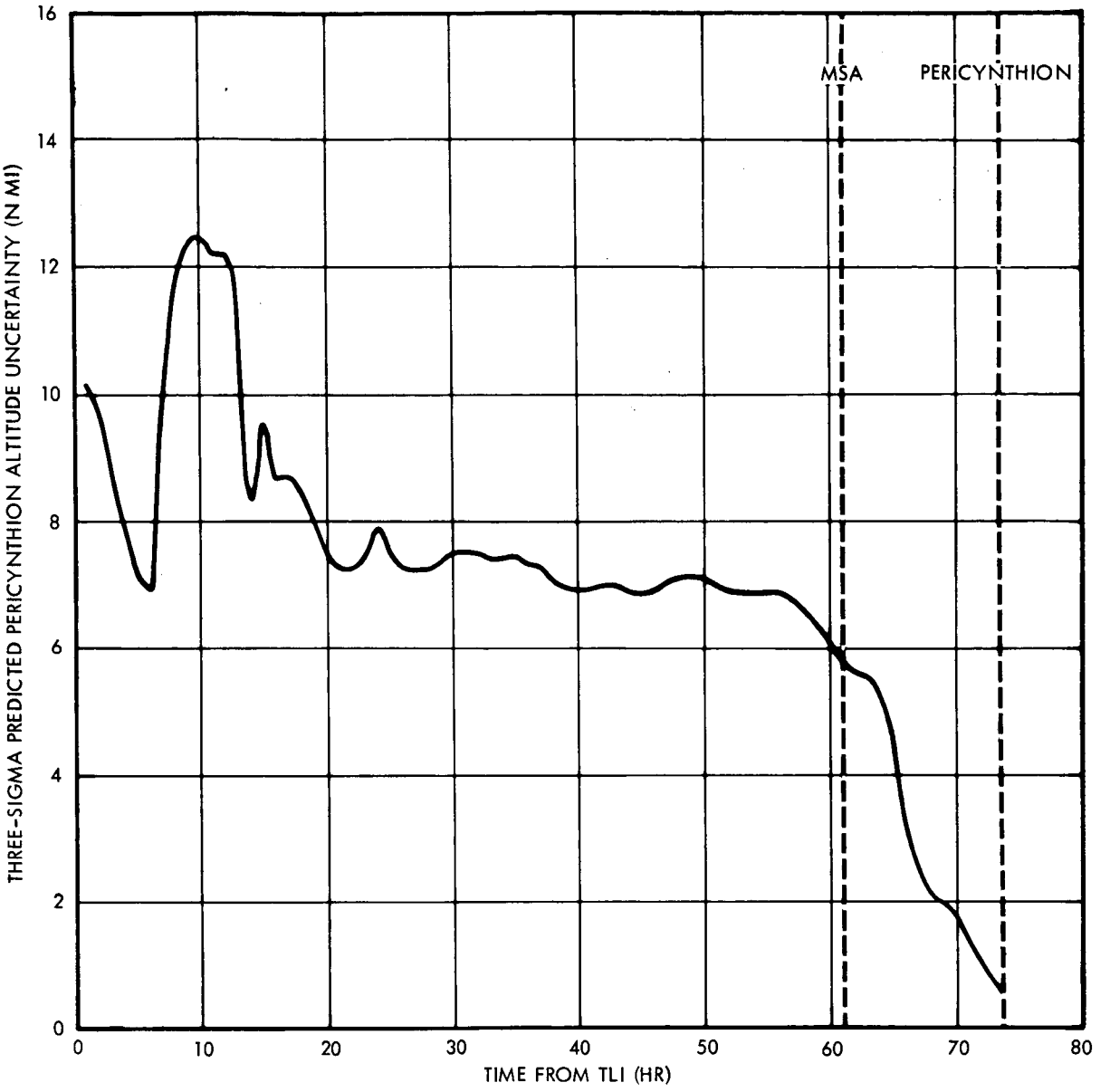

Figure 7. Three-Sigma Predicted Pericynthion Altitude Uncertainty - Translunar Phase

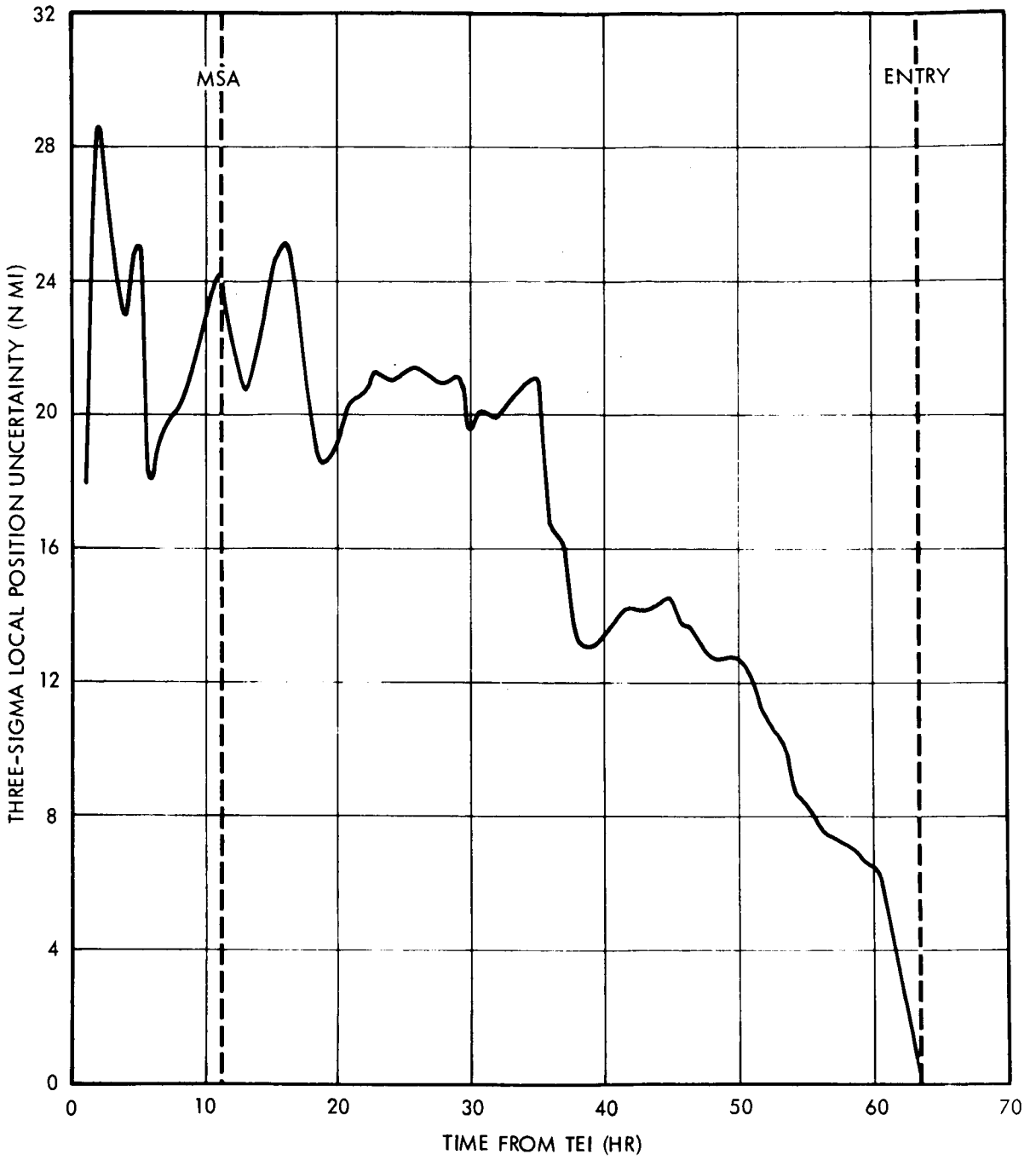

Figure 8. Three-Sigma Local Position Uncertainty - Transearth Phase

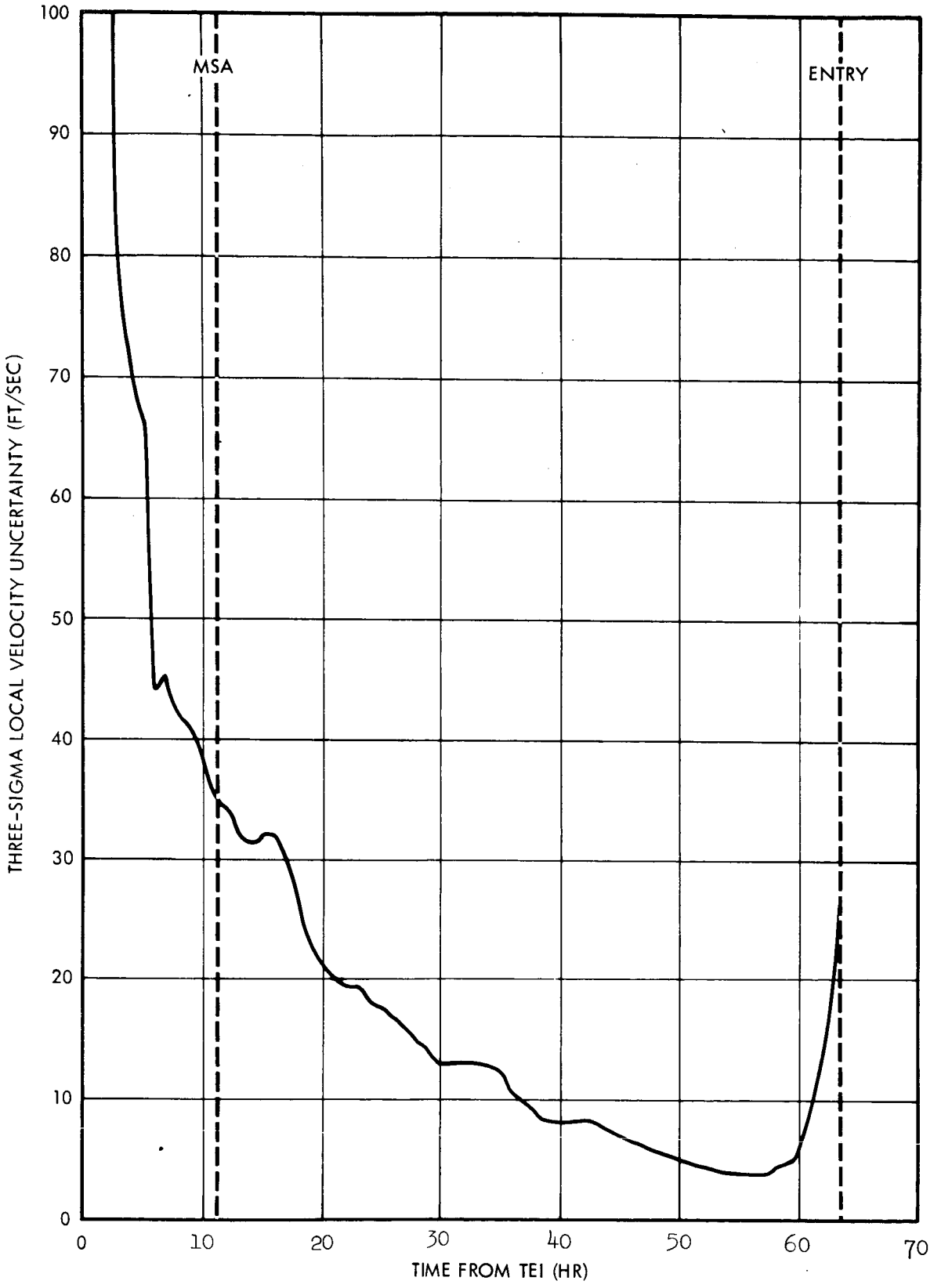

Figure 9. Three-Sigma Local Velocity Uncertainty - Transearth Phase

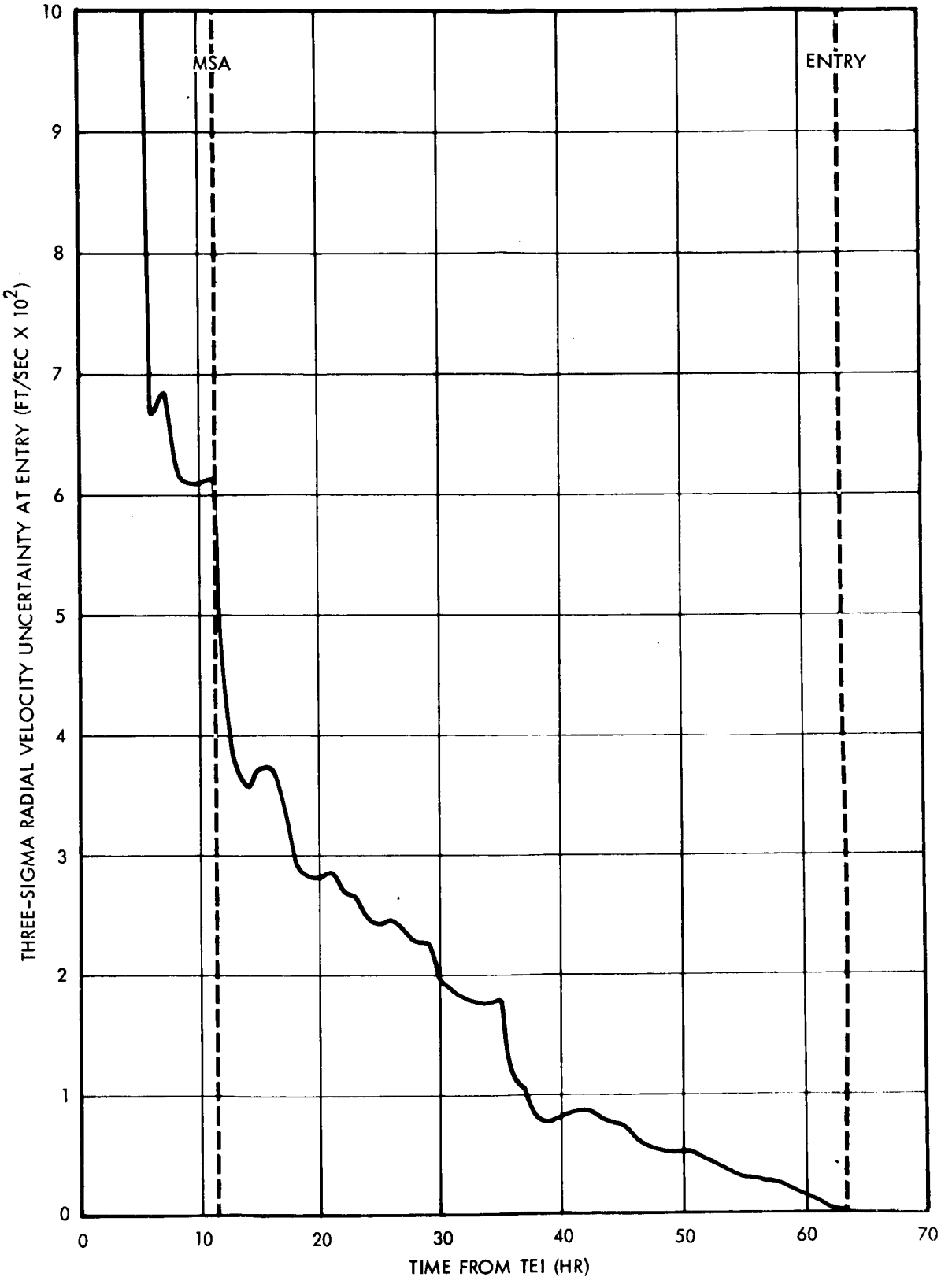

Figure 10. Three-Sigma Predicted Radial Velocity Uncertainty at Entry - Transearth Phase

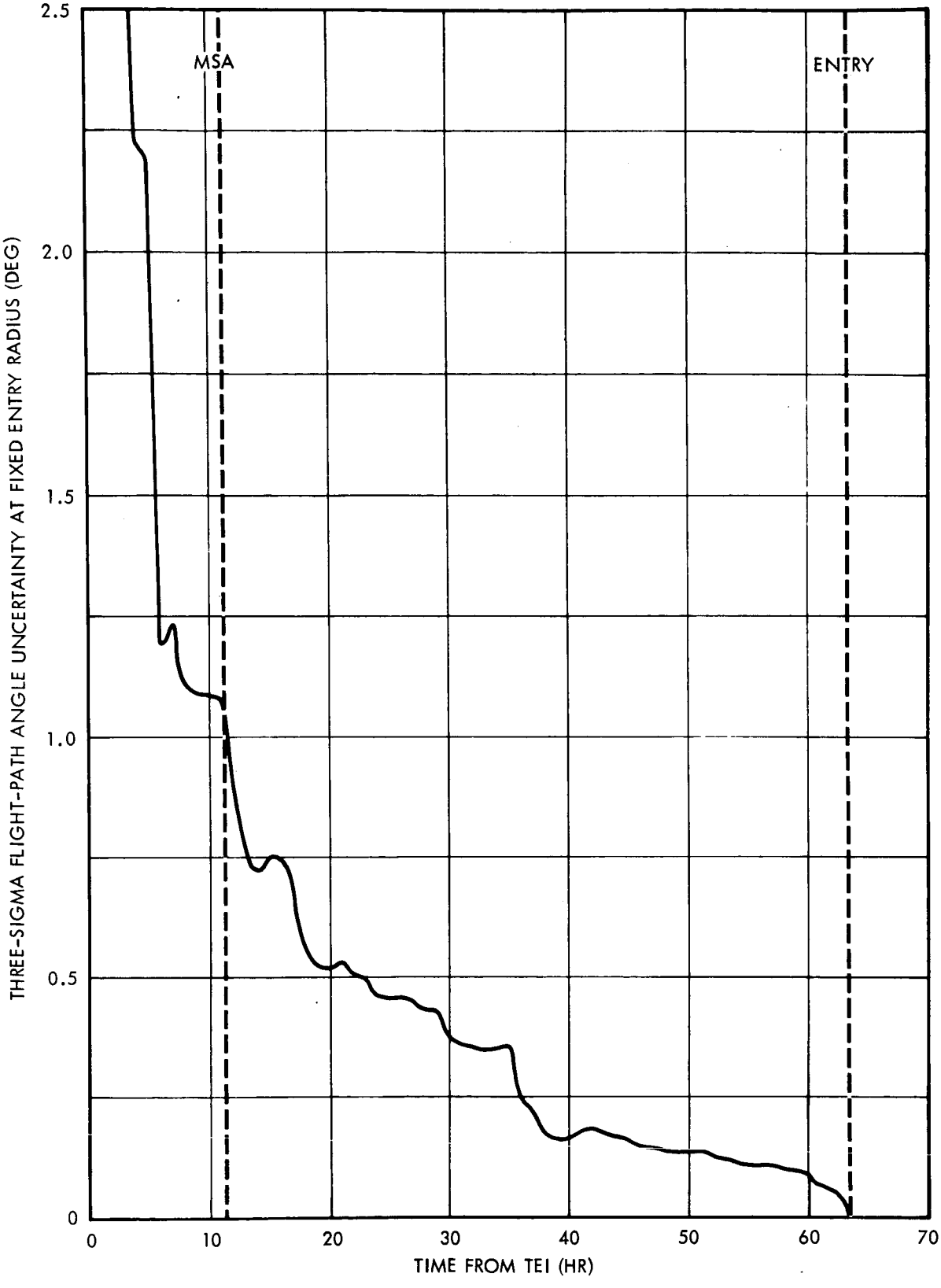

Figure 11. Three-Sigma Predicted Flight-Path Angle Uncertainty at Fixed Entry Radius - Transearth Phase

REFERENCES

1. Preliminary Apollo Mission F Trajectory Data for the May 1969 Launch Window. MSC Internal Note No. 69-FM-27, January 28, 1969.

2. TAPP-IV Programming Description. TRW-68-FMT-612, May 15, 1968.

3. Hayman, L.: MOFIT, The Matrix Operations Formula Interpreter. July 1968.

4. Statistical Navigation Analysis Program (SNAP). TRW 69-FMT-732, February 10, 1969.

5. Bond, A. C.: TAPP-IV Passive Thermal Control Simulation for Task A-153.4. TRW IOC 3422.6-193, November 17, 1967.

6. RTCC Mission C′S-IVB LH_2 Venting Update. MSC Internal Note No. 68-FM-47-459, November 22, 1968.